Acta Cryst. (1996). A**52**, 471–475

Dynamical RHEED Calculations from the Surface of a Semi-Infinite Crystal

L.-M. PENG,[a]* S. L. DUDAREV[b] AND M. J. WHELAN[b]

[a]*Beijing Laboratory of Electron Microscopy, Chinese Academy of Sciences, PO Box 2724, Beijing 100080, People's Republic of China, and* [b]*Department of Materials, University of Oxford, Parks Road, Oxford OX1 3PH, England. E-mail: lmpeng@lmplab.blem.ac.cn*

(*Received 2 November 1995; accepted 25 January 1996*)

Abstract

A slab method for dynamical RHEED calculations from the surface of a semi-infinite crystal is developed. This method is based on an old idea of McRae [*Surf. Sci.* (1968), **11**, 479–491], who proposed that in LEED Bloch waves characterizing the bulk crystal may be obtained by diagonalizing the scattering matrix associated with a repeating bulk crystal slab. However, a direct implementation of this idea for dynamical RHEED calculation may result in divergent results. It is shown that this problem may be overcome by the method of Bethe potentials and the results obtained using the method of combined McRae and Bethe potentials are in good agreement with exact dynamical RHEED calculations.

1. Introduction

Many different methods for many-beam dynamical reflection high-energy electron diffraction (RHEED) calculations have been developed in recent years (Maksym & Beeby, 1981; Ichimiya, 1983; Peng & Cowley, 1986; Smith & Lynch, 1988; Zhao, Poon & Tong, 1988; Meyer-Ehmsen, 1989; Peng, Gjønnes & Gjønnes, 1992; Peng & Whelan, 1990; Rez, 1995). But all computation schemes except the Bloch-wave method (Bethe, 1928; Collela, 1972; Ma & Marks, 1989; Peng, 1989) deal with RHEED from the surface of a crystal slab having finite thickness, and for the convenience of the following discussion we will call methods of this type slab methods. On the one hand, the slab method provides the most efficient and accurate means for calculating reflected-beam intensities. But there exists many situations when accurate and simple expressions are needed for such quantities as the electron wave function within a semi-infinite bulk crystal, as in the case of surface phonon scattering (Dudarev, Peng & Whelan, 1993), and these expressions are not readily obtainable by the slab method. On the other hand, although in principle the Bloch-wave method is applicable for RHEED from the surface of a three-dimensionally periodic crystal, it is not easy to deal with a selvedge and to obtain convergent results. Methods have been proposed to combine the slab method and the Bloch-wave method (see, for example, Peng, 1994) but, nowadays, with state-of-the-art numerical routines of matrix diagonalization (NAG, 1993), this combination has yet to compete with the slab method both in efficiency and in accuracy. In this paper, we will develop a slab method that is capable of calculating dynamical RHEED from the surface of a semi-infinite crystal and show that our method is efficient and agrees well with the ordinary slab method.

Our method is based on an old idea of McRae (1968), who first pointed out that the dynamical low-energy electron diffraction (LEED) problem and the corresponding band-structure problem for the substrate may be reduced to a matrix eigenvalue problem involving the scattering matrix for a substrate layer. While this approach has been successfully applied for dynamical LEED calculations (see, for example, Stampfl, Kambe, Riley & Lynch, 1992), a direct implementation of McRae's idea into dynamical RHEED theory results in divergent results (see §2 below). This is because in dynamical LEED calculations the effective pseudo-potential is much less localized than in the RHEED case. A small number of Fourier coefficients of the pseudo-potential is normally sufficient for the description of LEED, while in RHEED a larger number of Fourier coefficients are required. In §2, we will first discuss how McRae's idea can be implemented into dynamical RHEED theory and then show that the problem of divergence may be overcome by the use of the method of Bethe potentials. In §3, a numerical example will be given to demonstrate the use of the method outlined in §2 for dynamical RHEED calculations from the surface of a semi-infinite crystal.

2. Theory

It can be shown formally that all slab methods, including the ones by Maksym & Beeby (1981), Ichimiya (1983), Smith & Lynch (1986) and Peng & Whelan (1990), are equivalent, but differing essentially in their treatment of the relevant matrices. In the present paper, we use the method described in Peng & Whelan (1990).

Briefly, in a periodic bulk crystal we have

$$\Psi(z+c) = \mathbf{M}(c)\Psi(z), \tag{1}$$

where $\Psi(z)$ is a super vector as given by

$$\Psi(z) = \begin{pmatrix} \Psi_G(z) \\ -i\Psi'_G(z) \end{pmatrix}, \tag{2}$$

in which $\Psi_G(z)$ is the diffracted-beam amplitude associated with the Gth rod of the reciprocal lattice and Ψ'_G is its surface normal derivative. The matrix $\mathbf{M}(c)$ appearing in (1) is called the scattering matrix and the constant c is the lattice constant along the surface-normal direction.

For a Bloch wave $b(\mathbf{r})$ in a crystal, it can be readily shown that both the Gth component b_G and its surface-normal derivative $b'_G = \mathrm{d}(b_G)/\mathrm{d}z$ satisfy the Bloch theorem

$$\begin{aligned} b_G^{(j)}(z+c) &= \exp(i\gamma^{(j)}c)b_G^{(j)}(z), \\ b_G'^{(j)}(z+c) &= \exp(i\gamma^{(j)}c)b_G'^{(j)}(z) \end{aligned} \tag{3}$$

and that they are therefore both Bloch waves. We define a super vector $\mathbf{b}^{(j)}$ by

$$\mathbf{b}^{(j)} = \begin{pmatrix} b_G^{(j)} \\ -ib_G^{(j)} \end{pmatrix}. \tag{4}$$

Since (1) holds for a general wave function, it also holds for $\mathbf{b}^{(j)}$ defined by (4), *i.e.*

$$\mathbf{b}^{(j)}(z+c) = \exp(i\gamma^{(j)}c)\mathbf{b}^{(j)}(z) = \mathbf{M}(c)\mathbf{b}^{(j)}(z), \tag{5}$$

in which $\gamma^{(j)}$ is the jth eigenvalue associated with the jth super vector $\mathbf{b}^{(j)}(z)$.

For a dynamical RHEED calculation involving n reciprocal-lattice rods, the scattering matrix $\mathbf{M}$ is a $2n \times 2n$ matrix. In general, this $2n \times 2n$ matrix will give a total of $2n$ Bloch waves, of which n propagate downwards into the crystal slab, and in the presence of absorption decay in amplitude downwards. The other n propagate and decay in the reverse direction. By introducing a $2n \times 2n$ matrix $\mathbf{C} = (\mathbf{b}^{(1)}, \cdots, \mathbf{b}^{(2n)})$ and a diagonal matrix $\boldsymbol{\Upsilon}(z) = \{\exp(i\gamma^{(j)}z)\}$, we then have

$$\mathbf{M}(z) = \mathbf{C}\boldsymbol{\Upsilon}(z)\mathbf{C}^{-1}. \tag{6}$$

For a crystal slab consisting of m repeating unit slabs, substitution of (6) into (1) gives

$$\boldsymbol{\Psi}(z+mc) = \mathbf{C}\boldsymbol{\Upsilon}(mc)\mathbf{C}^{-1}\boldsymbol{\Psi}(z). \tag{7}$$

Without loss of generality, we can assume that among the total $2n$ Bloch waves the first n Bloch waves are evanescent waves and the remaining waves are anti-evanescent. For a semi-infinite crystal, these anti-evanescent Bloch waves are not physically allowed and must be discarded. Assuming that the interface between the selvedge and the bulk crystal is at $z = z_s$ and that the scattering matrix associated with the selvedge is $\mathbf{M}_s$, we then have for a crystal slab consisting of m repeating unit slabs

$$\begin{aligned} \boldsymbol{\Psi}(z+mc) &= \mathbf{C}\boldsymbol{\Upsilon}(mc)\mathbf{C}^{-1}\mathbf{M}_s\boldsymbol{\Psi}(0) \\ &= \mathbf{C}\begin{pmatrix} \{\exp(i\gamma^{(i)}mc)\} & \\ & \{\exp(i\gamma^{(i+n)}mc)\} \end{pmatrix} \\ &\quad \times \mathbf{C}^{-1}\mathbf{M}_s\begin{pmatrix} \{\delta_{G0} + \mathcal{R}_G\} \\ \{k_{G_z}(\delta_{G0} - \mathcal{R}_G)\} \end{pmatrix}, \end{aligned} \tag{8}$$

in which $\mathcal{R}_G$ is the reflected-beam amplitude associated with the Gth reciprocal-lattice rod.

For a semi-infinite crystal, since all physically allowed quantities must have a finite amplitude, the lower half of the column vector $\mathbf{C}^{-1}\mathbf{M}_s\boldsymbol{\Psi}(0)$ on the right-hand side of (8) must vanish. In terms of the two lower submatrices $\mathbf{M}'_{21}$ and $\mathbf{M}'_{22}$ of the matrix $\mathbf{M}' = \mathbf{C}^{-1}\mathbf{M}_s$ and the surface reflected-beam-amplitude vector $\{\mathcal{R}_G\}$, we can write the condition as

$$M'_{21}\{\delta_{G0} + \mathcal{R}_G\} + M'_{22}\{k_{G_z}(\delta_{G0} - \mathcal{R}_G)\} = 0, \tag{9}$$

which gives

$$R_G = -\left(\{M'_{21} - M'_{22}k_{H_z}\}_{GH}\right)^{-1}\left(\{M'_{21} + M'_{22}k_{0_z}\}_{H0}\right). \tag{10}$$

To utilize (10) for dynamical RHEED calculations from the surface of a semi-infinite crystal, the scattering matrix $\mathbf{M}(c)$ associated with a repeating unit slab must first be calculated and then diagonalized by a similarity transformation as in (6). However, to achieve a convergent dynamical RHEED calculation, some evanescent beams must be included. The inclusion of evanescent beams, in particular positive higher-order Laue-zone (HOLZ) beams lying outside the Ewald sphere, usually gives rise to a divergent scattering matrix $\mathbf{M}(c)$ for a repeating unit slab, putting an upper limit on the number of evanescent beams that may be included in the calculation and consequently on the accuracy of the calculation.

The situation can be improved to a certain extent if the repeating unit slab of the substrate crystal consists of an assembly of identical layers of atoms, such as a monolayer of atoms, each having a thickness c and a relative shift $\mathbf{R}_t$ with respect to each other. The scattering matrix associated with the ith layer is then related to the $(i-1)$th layer by the relation

$$\mathbf{M}_i = \mathbf{Q}^{-1}\mathbf{M}_{i-1}\mathbf{Q} = (\mathbf{Q}^{-1})^{i-1}\mathbf{M}_0(\mathbf{Q})^{i-1}, \tag{11}$$

in which the matrix $\mathbf{Q}$ is a diagonal matrix with $\{Q\}_G = \exp(i\mathbf{G}\cdot\mathbf{R}_t)$, and $\mathbf{M}_0$ is the scattering matrix associated with the first layer. Following the general relation (1), we have

$$\begin{aligned} \boldsymbol{\Psi}(z+mc) &= \mathbf{M}_m\boldsymbol{\Psi}[z+(m-1)c] \\ &= \mathbf{M}_m\mathbf{M}_{m-1}\cdots\mathbf{M}_0\boldsymbol{\Psi}(z) \\ &= (\mathbf{Q}^{-1})^m(\mathbf{Q}\mathbf{M}_0)^m\boldsymbol{\Psi}(z). \end{aligned} \tag{12}$$

By a similarity transformation of the matrix $\mathbf{Q}\mathbf{M}_0$,

$$\mathbf{Q}\mathbf{M}_0 = \mathbf{C}\boldsymbol{\Upsilon}\mathbf{C}^{-1}, \tag{13}$$

we obtain

$$\boldsymbol{\Psi}(z+mc) = (\mathbf{Q}^{-1})^m\mathbf{C}\boldsymbol{\Upsilon}(mc)\mathbf{C}^{-1}\boldsymbol{\Psi}(z). \tag{14}$$

This expression is similar to (7) and, following a similar argument to that leading to (10), we obtain an identical expression for the reflected-beam-amplitude vector (10). Since the thickness of a layer of atoms is smaller than that of a repeating unit slab, the validity of the above procedure is improved compared with that using a repeating unit slab.

For a selvedge with a simple structure, the scattering matrix $\mathbf{M}_s$ associated with the surface selvedge can be simple and convergent if the scattering matrix associated with the bulk slab $\mathbf{M}(c)$ is convergent. However, for a complicated surface structure, the thickness of the selvedge could be larger than that of a bulk slab and its scattering matrix $\mathbf{M}_s$ could be divergent even if that associated with the bulk slab is convergent. In this case we can propagate a so-called **R** matrix (Ichimiya, 1983; Zhao *et al.*, 1988) rather than the scattering matrix through the selvedge. Assuming that the whole crystal system consists of a total of m bulk slabs and the selvedge interface is at $z = z_s$, we have then the following expression for relating the super vector at the bottom of the whole crystal system to that at the selvedge interface

$$\Psi(z_s + mc) = \mathbf{C}\Upsilon(mc)\mathbf{C}^{-1}\Psi(z_s). \tag{15}$$

By writing

$$\mathbf{C}^{-1} = \mathbf{C}' = \begin{pmatrix} \mathbf{C}'_{11} & \mathbf{C}'_{12} \\ \mathbf{C}'_{21} & \mathbf{C}'_{22} \end{pmatrix}, \tag{16}$$

and following the same procedure leading to (9), we obtain

$$\mathbf{C}'_{21}\{\Psi_G(z_s)\} + \mathbf{C}'_{22}\{-i\Psi'_G(z_s)\} = 0, \tag{17}$$

which gives the **R** matrix at the selvedge interface,

$$\mathbf{R} = -(\mathbf{C}'_{22})^{-1}(\mathbf{C}'_{21}), \tag{18}$$

that relates the surface-normal derivative of the wave-function vector $\{\Psi'_G\}$ and the wave-function vector $\{\Psi_G\}$

$$\{-i\Psi'_G(z)\} = \mathbf{R}\{\Psi_G(z)\}. \tag{19}$$

This **R** matrix can then be propagated upwards to the surface to give the required surface reflected-beam amplitudes (Peng, 1994).

When the solid is composed of moderately strong scattering atoms, the scattering matrix associated with even a monolayer of atoms can be divergent. The problem arises from the inclusion of the evanescent beams lying outside the Ewald sphere. It has now been well established that, although each of these strong evanescent waves contributes little to the resulting RHEED rocking curves, in general their collective contribution is not negligible.

In principle, the problem of dynamical RHEED involves an infinite number of rods of the reciprocal lattice. However, since the scattering power of the crystal is effectively band-width limited, only a finite set of reciprocal-lattice rods, say N rods, are needed for the description of the main features of RHEED. Artificially, we may divide the N rods of the reciprocal lattice into two groups, one referring to the strong beams and the other to the weak beams, based on the quantity $\Gamma_H^2 = K^2 - |\mathbf{K}_t + \mathbf{H}|^2$ associated with the beams, where **K** is the incident electron wave vector corrected for the mean inner potential and the subscript t denotes the tangential component of the wave vector. For weak beams, we have the inequality $|\Gamma_H^2 - K_z^2| >> |U_{\max}|$, where $|U_{\max}|$ is the maximum of all $|U_{H'}|$ for weak beams, while for strong beams this inequality is not satisfied. If both groups of beams are treated fully in the dynamical RHEED theory, then, roughly speaking, for weak beams there exists a one-to-one correspondence between Bloch waves and the reciprocal-lattice rods, and for these Bloch waves we have approximately $\gamma^{(i)2} \simeq \Gamma_H^2$. For evanescent beams, we have $\gamma^{(i)} \simeq \pm i|\Gamma_H|$. From (8), it is clear that the scattering matrix **M** associated with a crystal slab then contains terms of the form $\exp(|\Gamma_H|c)$. For a given value of the slab thickness c, we then have an upper limit $\Gamma_{\max}$ on $|\Gamma_H|$, *i.e.* all weak beams with $|\Gamma_H| > \Gamma_{\max}$ cannot be included in the calculation. Extensive computations confirmed that the inclusion of beams with $|\Gamma_G| < \Gamma_{\max}$ is usually not sufficient to produce convergent results.

At this stage, we note that, in the method of Bethe potentials (Bethe, 1928; Ichimiya, 1988; Peng, Dudarev & Whelan, 1996), beams with sufficiently large values of $|\Gamma_H|$ may be treated as a perturbation. Justification for the use of the Bethe potential method is that for an N-rod RHEED case, among the total of $2N$ Bloch waves only a smaller set of $2n$ ($n \leq N$) Bloch waves are important and have appreciable excitation amplitudes. Although all N rods of the reciprocal lattice are needed to give correct eigenvalues and eigenvectors for these $2n$ important Bloch waves, only n reciprocal-lattice rods need to be treated fully, while the effect of the remaining $N-n$ rods may be taken into account as a perturbation. We have found that the method of Bethe potentials works well in this respect. In the next section, we will show that the upper limit imposed on $|\Gamma_H|$ for evanescent beams by the condition that the scattering matrix **M** must be finite and the low limit set by the Bethe approximation overlap. The divergence problem encountered in diagonalizing the scattering matrix **M** is then solved by the use of the Bethe potential method.

3. Numerical results

In this section, we will present some results for the Ag (001) surface. The high-energy electrons are incident on the surface along the [110] azimuth. For convenience,

we will use an index system that the conventional [110] beam azimuth corresponds to [10]. Using this indexing notation, the zero-order Laue-zone (ZOLZ) beams $(n, \bar{n}, 0)$ can be simply written as $(0, n)$ and the HOLZ beams $(n+m, \bar{n}+m, 0)$, where m refers to the order of the HOLZ zones, is written as (m, n). The primary-beam energy used in the following calculation is 20 keV and the complex atomic scattering factors are taken from Dudarev, Peng & Whelan (1995).

Shown in Fig. 1 is a calculated kinematic RHEED pattern using *CERIUS*[2] of MSI. While it is well known that for RHEED geometry the kinematic theory does not give the right intensity, this kinematic diffraction pattern nevertheless gives the correct diffraction geometry. The two diffraction rings consist of diffraction spots of the type $(0, n)$ and $(\bar{1}, n)$ are ZOLZ and first negative HOLZ zones, respectively, and all positive HOLZ beams are evanescent and not visible in the RHEED pattern.

Shown in Fig. 2 are dynamical RHEED rocking curves for the specular (00) and (01) beams. The curve with the key '16 rod calculation' was calculated using nine ZOLZ beams $(0,0)$, $(0,\pm1)$, $(0,\pm2)$, $(0,\pm3)$, $(0,\pm4)$ and seven HOLZ beams $(-1, 0)$, $(-1,\pm1)$, $(-1,\pm2)$, $(-1,\pm3)$ and using (10). When higher-order ZOLZ beams and other HOLZ beams are included, the scattering matrix $\mathbf{M}(c)$ becomes divergent. However, the curve with the key 'full 33 rod calculation' in the figure shows clearly that the 16-rod calculation is not convergent. This 33-rod calculation uses the same 16 rods of the reciprocal lattice as in the earlier curve, but includes an additional 17 HOLZ beams and uses the conventional RHEED slab method (Peng & Whelan, 1990) rather than the method discussed in §2. These additional beams are $(-2,0)$, $(-2,\pm1)$, $(-2,\pm2)$, $(1,0)$, $(1,\pm1)$, $(1,\pm2)$, $(1,\pm3)$, $(2,0)$, $(2,\pm1)$, $(2,\pm2)$. The third curve in the figure with the key '16 rod + Bethe potentials' was calculated using the basic set of 16 rods as in other curves, and the remaining 21 rods were treated using the method of Bethe potentials (see Peng *et al.*, 1996, for details). Fig. 2 shows that, while the 16-rod calculation differs substantially from the full 33-rod calculation, the use of Bethe potentials produces almost perfect results. To be more quantitative, we have calculated a so-called R factor defined as

$$R_{AB} = \sum_i |I_A - I_B|/I_A, \tag{20}$$

in which I_A and I_B denote intensities of curves A and B, and the index i refers to the ith data point. For the specular (00) beam, $R = 0.53$ between curves of the full 33-rod calculation and the 16-rod calculation, $R = 0.0085$ between the full 33-rod calculation and the 16-rod curve with Bethe potentials. For the (01) rod, the values for the two cases are 0.90 and 0.015, respectively. These figures demonstrate clearly that the use of Bethe potentials greatly improves the accuracy of the approximate calculation using only a limited set of beams and equation (10).

4. Conclusions

In this paper, a slab method is developed for calculating dynamical RHEED from the surface of a semi-infinite crystal. This method combines the usual slab method of RHEED with the method of Bethe potentials. Our results show that this method is efficient and convergent and they agree well with those calculated using the conventional slab method.

This work was supported by the Chinese Academy of Sciences and National Natural Science Foundation of China (LMP), the Engineering and Physical Science

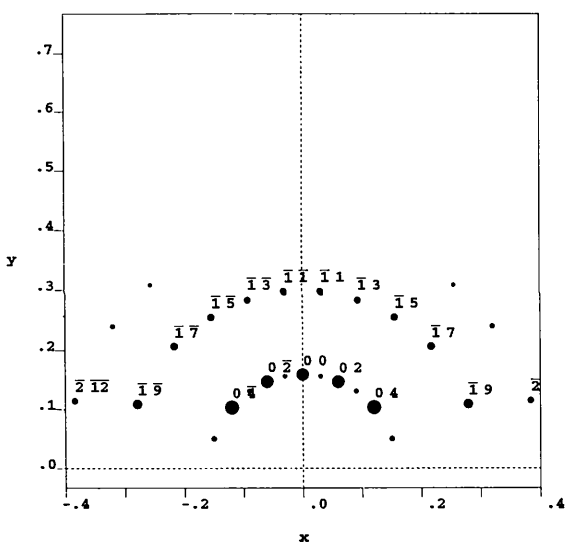

Fig. 1. Kinematic RHEED pattern calculated for 20 keV primary-beam energy and an Ag (001) surface for the [110] beam azimuth.

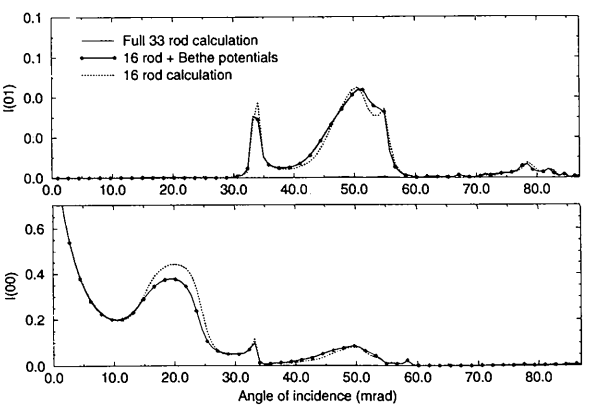

Fig. 2. Dynamical RHEED rocking curves calculated from an Ag (100) surface. The calculations are made for 20 keV primary-beam energy and 293 K, and the two graphs are for the specular (00) beam and a side (01) beam.

Research Council (EPSRC) (grant no. GR/H96423) and the Royal Society (Joint Project no. Q711).

References

Bethe, H. (1928). *Ann. Phys. (Leipzig)*, **87**, 55–129.
Colella, R. (1972). *Acta Cryst.* A**28**, 11–15.
Dudarev, S. L., Peng, L.-M. & Whelan, M. J. (1993). *Proc. R. Soc. London Ser. A*, **440**, 567–588.
Dudarev, S. L., Peng, L.-M. & Whelan, M. J. (1995). *Surf. Sci.* **330**, 86–100.
Ichimiya, A. (1983). *Jpn. J. Appl. Phys.* **22**, 176–180.
Ichimiya, A. (1988). *Acta Cryst.* A**44**, 1042–1044.
Ma, Y. & Marks, L. D. (1989). *Acta Cryst.* A**45**, 174–182.
McRae, E. G. (1968). *Surf. Sci.* **11**, 479–491.
Maksym, P. A. & Beeby, J. L. (1981). *Surf. Sci.* **110**, 423–438.
Meyer-Ehmsen, G. (1989). *Surf. Sci.* **219**, 177–188.
NAG (1993). *NAG Fortran Library Manual.* NAG Ltd, Oxford, England.
Peng, L.-M. (1989). *Surf. Sci.* **222**, 296–312.
Peng, L.-M. (1994). *Advances in Imaging and Electron Physics*, Vol. 90, edited by P. W. Hawkes, pp. 205–351. New York: Academic Press.
Peng, L.-M. & Cowley, J. M. (1986). *Acta Cryst.* A**42**, 545–552.
Peng, L.-M., Dudarev, S. L. & Whelan, M. J. (1996). *Surf. Sci. Lett.* In the press.
Peng, L.-M., Gjønnes, K. & Gjønnes, J. (1992). *Microsc. Res. Tech.* **20**, 360–370.
Peng, L.-M. & Whelan, M. J. (1990). *Proc. R. Soc. London Ser. A*, **431**, 111–124, 125–142.
Rez, P. (1995). *Acta Cryst.* A**51**, 38–47.
Smith, A. E. & Lynch, D. F. (1988). *Acta Cryst.* A**44**, 780–788.
Stampfl, C., Kambe, K., Riley, J. D. & Lynch, D. F. (1992). *J. Phys. Condens. Matter*, **4**, 8461–8476.
Zhao, T. C., Poon, H. C. & Tong, S. Y. (1988). *Phys. Rev. B*, **38**, 1172–1195.